A review of high-speed electro-hydrostatic actuator pumps in aerospace applications: challenges and solutions

Qun Chao
State Key Laboratory of Fluid Power and Mechatronic Systems, Zhejiang University
No. 38 Zheda Road, Xihu District, Hangzhou 310027, China
chao_qun@zju.edu.cn

Junhui Zhang (Corresponding Author)
State Key Laboratory of Fluid Power and Mechatronic Systems, Zhejiang University
No. 38 Zheda Road, Xihu District, Hangzhou 310027, China
benzjh@zju.edu.cn

Bing Xu
State Key Laboratory of Fluid Power and Mechatronic Systems, Zhejiang University,
No. 38 Zheda Road, Xihu District, Hangzhou 310027, China
bxu@zju.edu.cn

Hsinpu Huang
School of Mechanical Engineering, Zhejiang University
No. 38 Zheda Road, Xihu District, Hangzhou 310027, China
3140105119@zju.edu.cn

Min Pan
Department of Mechanical Engineering, University of Bath,
Bath BA2 7AY, Avon, UK
M.Pan@bath.ac.uk

Abstract The continued development of electro-hydrostatic actuators (EHAs) in aerospace applications has put forward an increasing demand upon EHA pumps for their high power density. Besides raising the delivery pressure, increasing the rotational speed is another effective way to achieve high power density of the pump, especially when the delivery pressure is limited by the strength of materials. However, high-speed operating conditions can lead to several challenges to the pump design. This paper reviews the current challenges including the cavitation, flow and pressure ripples, tilting motion of rotating group and heat problem, associated with a high-speed rotation. In addition, potential solutions to the challenges are summarized, and their advantages and limitations are analyzed in detail. Finally, future research trends in EHA pumps are suggested. It is hoped that this review can provide a full understanding of the speed limitations for EHA pumps and offer possible solutions to overcome them.

Key words: Electro-hydrostatic actuator (EHA); EHA pump; High-speed pump; Cavitation; Flow and pressure ripples; Tilting motion; Heat problem

1. Introduction

Flight controls in an aircraft can be typically divided into two types: primary flight control and secondary flight control [1,2]. The primary flight control is responsible for controlling the roll, yaw and pitch attitudes and the trajectory of the aircraft, while the second flight control is used to control the lift of the wing. The flight control surfaces usually include ailerons, rudders, elevators, horizontal stabilizer, spoilers, leading edge slats and trailing edge flaps. Most of them in in-service military and commercial aircrafts are actuated by centralized hydraulic systems where the electric or engine-driven pumps provide pressurized hydraulic fluids for the hydraulic actuators [3] .

The electro-hydrostatic actuator (EHA) is an emerging aerospace technology that aims to replace the centralized hydraulic systems by self-contained and localized direct-drive actuator systems [2]. The EHA first replaced the F-18 standard left aileron actuator in 1997 and was evaluated throughout the Systems Research Aircraft flight envelope [4]. The ground and flight test results showed that the EHA could perform as well as the replaced actuator, and the stiffness, accuracy and bandwidth were sufficient for the application of EHAs on primary flight control surfaces. Recently, the EHAs have been integrated into the F-35 flight control actuation system to power its primary and secondary flight control

surfaces including horizontal tails, flaperons, rudders and leading edge flaps [5,6]. On the civil aircraft side, the EHAs have entered into service in the famous Airbus aircraft A380 since 2004, and they are normally used as backup actuators for some flight control surfaces, such as elevators, ailerons, rudders and spoilers [1]. Since then, the EHAs have been successfully applied to other civil aircrafts, such as A400M and A350 [7].

The aircraft benefits greatly from the replacement of centralized hydraulic systems with EHA systems [2,8,9]. Firstly, the EHA system has higher energy efficiency because it consumes power only when the control surfaces need to be actuated. Secondly, the EHA system adopts power-by-wire (PBW) technology and requires only electrical energy input, which offers weight savings due to the removal of conventional hydraulic systems. Thirdly, EHAs are much easier to remove and install than conventional hydraulic actuators, thus improving the maintainability. Finally, the EHA system has a higher degree of survivability/robustness because individual EHAs are parallel with each other.

A typical EHA system mainly consists of a bi-directional electric motor, a bi-directional pump, a symmetrical hydraulic actuator and a bypass valve [8,10], as shown in **Fig. 1a**. The electric motor drives the pump which provides pressurized fluid for the hydraulic actuator. The pump used in the EHA system is often called EHA pump, and it is usually an axial piston pump [11]. The configuration of a typical axial piston pump is shown in **Fig. 1b**. The whole rotating group is supported by two bearings at shaft ends and is submerged by the fluid medium in the pump casing. The cylinder block is coupled with the shaft through a spline mechanism. A compressed spring is installed in the cavity to push the cylinder block against the valve plate. In general, an odd number of piston-slipper assemblies are nested within the cylinder block at equal angular intervals about the centerline of the cylinder block. The piston is connected to the slipper at the head via a ball-and-socket joint. The slipper slides on the swash plate and a reasonable gap height between them is kept by a retainer (not shown in **Fig. 1b**). The inclined swash plate forces the multiple piston-slipper assemblies to reciprocate within the cylinder block, thereby generating a displacement chamber. The low-pressure fluid enters the displacement chamber from one valve plate opening as the piston experiences a suction stroke, while the high-pressure fluid is discharged from the displacement chamber to the other valve plate opening as the piston experiences a delivery stroke. The above motions repeat themselves for each shaft revolution and thus realizing a conversion from mechanical energy to hydraulic energy.

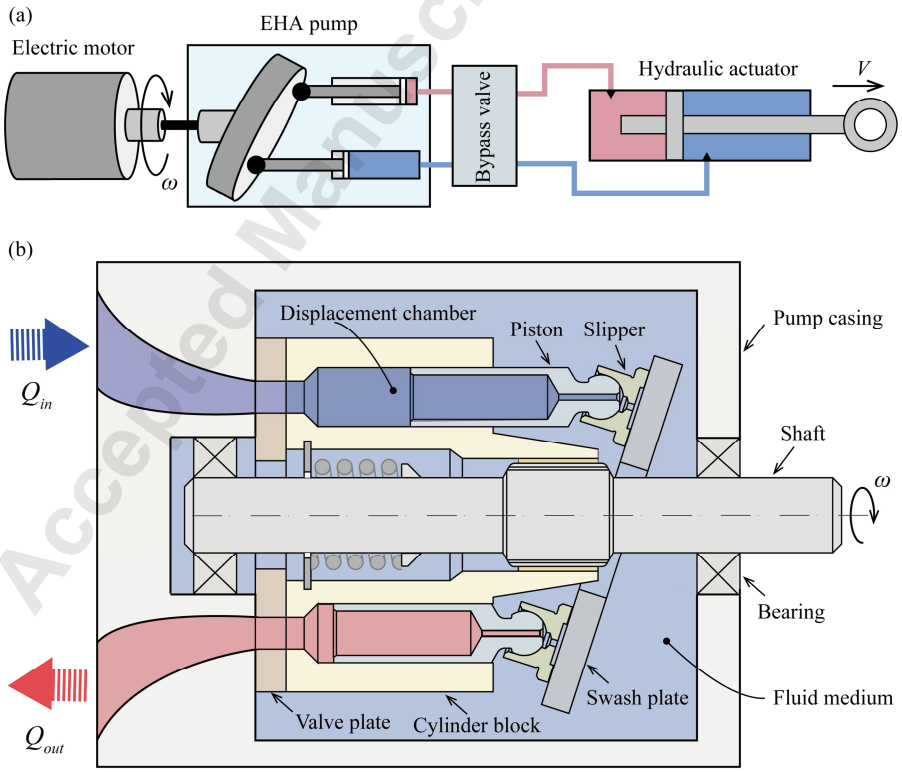

Fig. 1 The axial piston pump used in the EHA system: (a) schematic of an EHA system; (b) schematic of an axial piston pump

In aerospace applications, a high power density (power to weight ratio) is a crucial requirement for EHA pumps. It is an effective way to improve the power density of EHA pumps by increasing the rotational speed. **Figure 2** shows a relationship between a maximum rotational speed and a volumetric displacement [12]. It can be seen from **Fig. 2** that a higher maximum rotational speed goes along with the possibility to scale down the pump size and weight, which can increase the power density. This scale-down effect is significant for relatively low rotational speeds but becomes less positive when the rotational speed is higher than 10,000 r/min. Generally, the rotational speed of EHA pumps in aerospace applications is required to be more than 10,000 r/min [13] at which the pump displacement is estimated to be less than 5 mL/r from the fitting curves in **Fig. 2**. A further reduction of the pump displacement would lead to a striking increase of the rotational speed. However, in practice the rotational speed of EHA pumps is limited by various mechanical restrictions, which is adverse to the power density of EHA pumps.

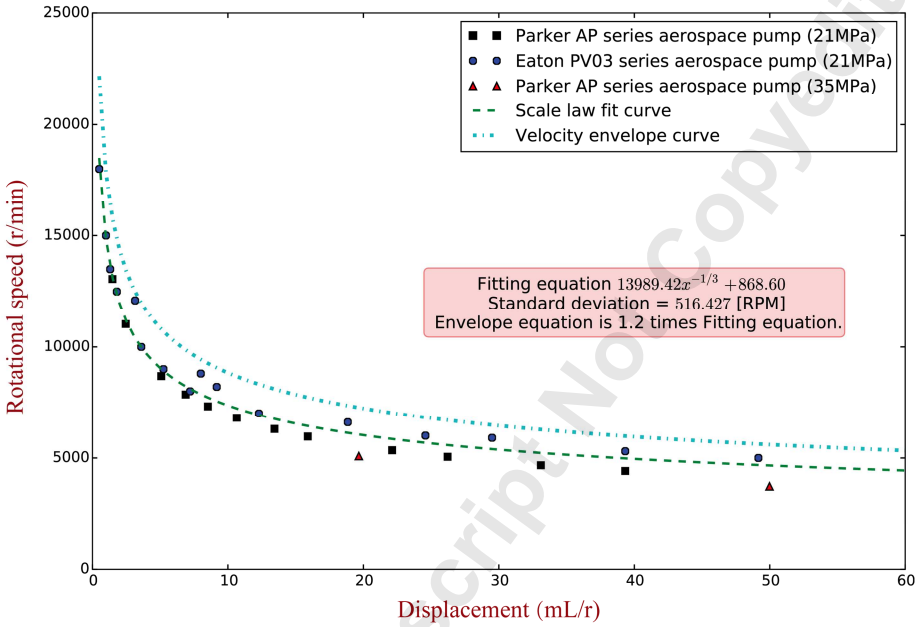

Fig. 2 Relationship between a maximum rotational speed and a volumetric displacement for three different aerospace pumps [12]

This paper aims to review the relevant publications in the field of axial piston pump in order to highlight the challenges associated with high-speed rotation. In addition, possible solutions to the challenges are also suggested and discussed. The rest of this paper is organized as follows: section 2 elaborates about the cavitation problem; section 3 includes the flow and pressure ripples; section 4 deals with the tilting motion of rotating group; section 5 describes the heat problem; finally, conclusions are presented in section 6.

2. Cavitation

Cavitation describes the dynamic process of cavity generation in a liquid [14], which includes two forms in terms of the formation mechanism of bubbles: gaseous cavitation and vaporous cavitation. The gaseous cavitation occurs when the oil pressure is lower than the saturation pressure of the gas. At this point, the dissolved gas releases from the solution and forms bubbles. When the localized fluid pressure becomes lower than the vapor pressure, the vaporous cavitation happens. At this time, the fluid vaporizes and forms vapor bubbles. In most hydrostatic machines, the gaseous cavitation takes places more commonly than the vaporous cavitation because the vapor pressure of the oil is much lower than the saturation pressure of the gas [15,16].

There are four main factors leading to the cavitation as the result of a sufficient pressure drop. The first factor is about the excessive pressure losses due to the flow resistance [17,18]. As the piston is pulled out of the cylinder block during the suction phase, the increased void volume in the cylinder chamber needs to be filled by sufficient inlet fluid flow. The supplied fluid travels from the pump inlet to the valve plate opening, consuming a portion of inlet pressure. Another inlet

pressure is consumed when the entering fluid undergoes a contraction of flow passage from the valve plate opening to the rotating cylinder port [19–21] and an enlargement of flow passage from the cylinder port to the cylinder chamber [14,22]. In addition, much inlet pressure is consumed as the cylinder fluid needs to be accelerated again to the maximum velocity of the piston. The above total pressure drop will decrease the air solubility and produce an entrained air mixture if the inlet pressure is insufficient. This mixture of air and liquid oil is then supplied into the cylinder block, leading to the gaseous cavitation. Moreover, the vaporous cavitation could happen if the pressure losses are sufficient to reduce the localized pressure below the vapor pressure of the oil.

The second reason for cavitation is the pressure undershoot inside the cylinder chambers [23–28]. The reverse flow and trapping effect cause the pressure undershoot at the start of the suction stroke. In contrast, only the trapping effect causes the pressure undershoot at the end of the suction stroke. The pressure undershoot is almost increased proportionally to the rotational speed of the pump [26]. As a result, the transient cylinder pressure could drop below the gas or even vapor pressure at high speed, leading to gaseous or vaporous cavitation.

The third reason for cavitation is the high velocity jet flow formed in the relief groove of the valve plate, as shown in **Fig. 3a**. The high velocity jet flow results from the negative pressure gradient when the discharge pressure is initially greater than the cylinder pressure at the start of the discharge stroke [23,29–33]. As a result, the localized pressure could drop below the vapor pressure, leading to the cavitation near the relief groove and cylinder ports. Tsukiji *et al*. [31] designed a test pump with an acrylic cylinder block and used a high-speed video camera to visualize the jet flow near the relief groove of a valve plate from the perpendicular direction to the axis, as shown in **Fig. 3b**. The cavitation cloud was detected near the relief groove, which confirmed the cavitation occurrence due to the high velocity jet flow.

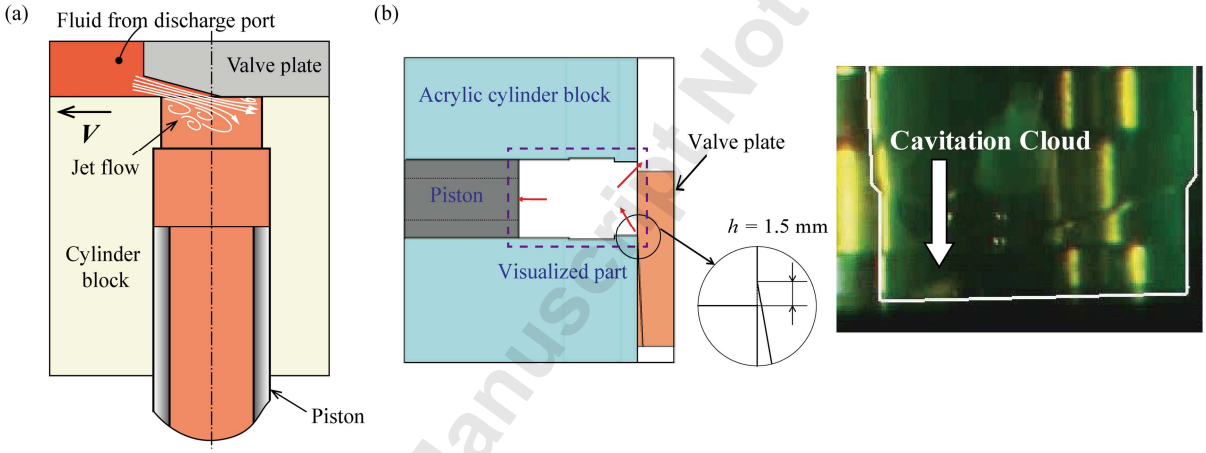

Fig. 3 Cavitation induced by the jet flow: (a) jet flow formed between the cylinder wall and relief groove of the valve plate; (b) detection of the cavitation [31]

Finally, the centrifugal force can also lead to cavitation in the cylinder chambers. During the phase of suction stroke, the centrifugal forces tend to push the "heavy" liquid towards the outside walls of the cylinder chambers but to leave the "light" air bubbles near the inside walls [20,34], as shown in **Fig. 4**. Consequently, the centrifugal effect produces a radially inhomogeneous pressure distribution in the cylinder chambers where the gaseous cavitation is most likely to occur near the inside walls of the cylinder chambers. In contrast, the gaseous cavitation is disappeared during the phase of discharge stroke because the cylinder pressure becomes high and the localized pressure drop due to the centrifugal effect is insufficient to cause gaseous cavitation.

Cavitation is harmful to the performance of EHA pumps. First, the gaseous cavitation reduces the cylinder filling that represents the ability of the cylinder block to receive hydraulic fluids from the pump inlet [21]. It can be seen from **Fig. 5** that when the rotational speed exceeds the rated rotational speed limit, the effective delivery flow rate starts to decline due to the occurrence of gaseous cavitation, which violates the flow continuity and reduces the volumetric efficiency of the pump [34–37].

In addition, the gaseous cavitation also reduces the fluid bulk modulus due to the released air bubbles [38–40], resulting in a delay of pressure build-up in the displacement chambers [15] and thus a slow response of the hydraulic cylinder to the varying load of the EHA system. When the air bubbles travel in the pump and encounter a high-pressure

region, they will collapse and bring about serious cavitation damage to the components, especially to the valve plate, cylinder block and slipper [15,36,41,42], as shown in **Fig. 6**. The cavitation erosion not only introduces contaminant particles into the working fluid and thus causing further abrasive wear, but also changes the geometries of sliding surfaces and thus damaging the sealing and bearing functions of lubricating interfaces. Besides, the collapse of the bubbles can increase the flow and pressure ripples, and the vibration and noise [32,43].

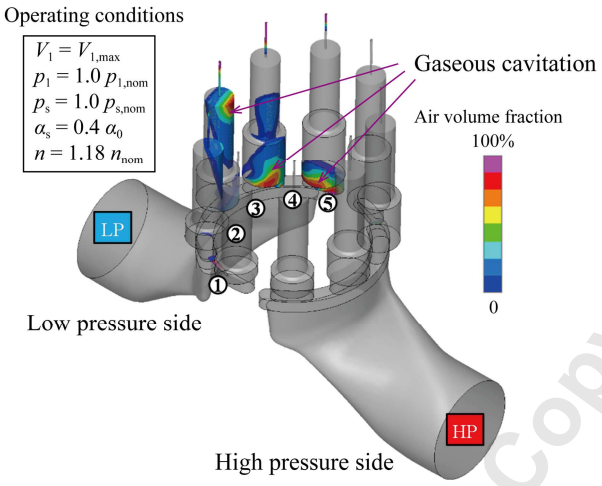

Fig. 4 Centrifugal effect on the cylinder pressure in the radial direction [34]

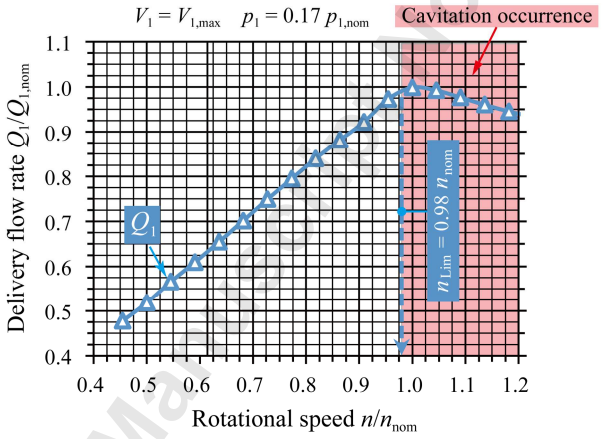

Fig. 5 Experimental results for the relationship between the delivery flow rate and the rotational speed [34]

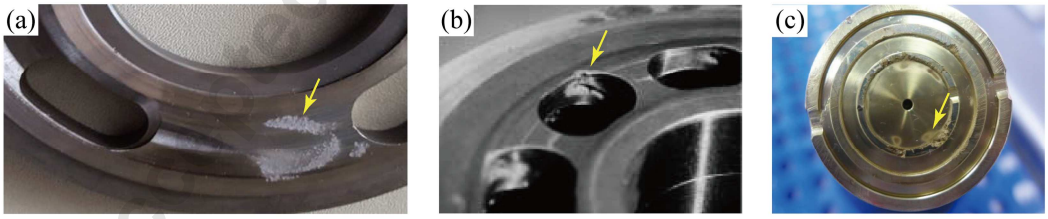

Fig. 6 Cavitation damage on the components of an axial piston pump: (a) valve plate [36], (b) cylinder block [41], (c) slipper

To prevent the cavitation occurrence within axial piston pumps, possible solutions have been investigated. Adding a boosting device is an effective way to increase the inlet pressure of the pump and thereby inhibit the cavitation [17,18,21,24,25,34,43,44]. For instance, the axial piston pump of Vickers® integrates an impeller at the end of the shaft to boost the suction pressure [44]. However, boosting the suction pressure can increase the air-borne noise [45], and the additional boosting device can cause parasitic losses and reduce the power density of the pump.

It is a preferred solution to improve the suction performance by optimizing the suction line because no additional

device is needed [46]. For instance, the novel design of meander-shaped suction ducts was reported to reduce pressure losses by more than 50 % for the flow from the pump inlet to the suction kidney [47]. Similarly, the revolution-oriented suction ducts were also considered to be able to reduce pressure losses by enabling the flow direction to match the circumferential velocity of the cylinder block as much as possible [48]. On the other hand, decreasing the circumferential velocity of the cylinder block is also a good solution to reduce pressure losses according to the Bernoulli equation [21]. As shown in **Fig. 7a**, the resultant velocity V of the hydraulic fluids entering the cylinder chamber consists of axial and circumferential components, V_{axial} and V_c. The circumferential velocity component is proportional to the pitch radius R of the cylinder ports, which means that the greater the pitch radius of the cylinder ports is, the higher the circumferential velocity component becomes. Compared with the standard flat design for the cylinder block bottom face, the spherical design allows a lower circumferential velocity of the hydraulic fluids entering the cylinder chamber [21,49] because it has a smaller pitch radius of the cylinder ports [50,51], as shown in **Fig. 7b**.

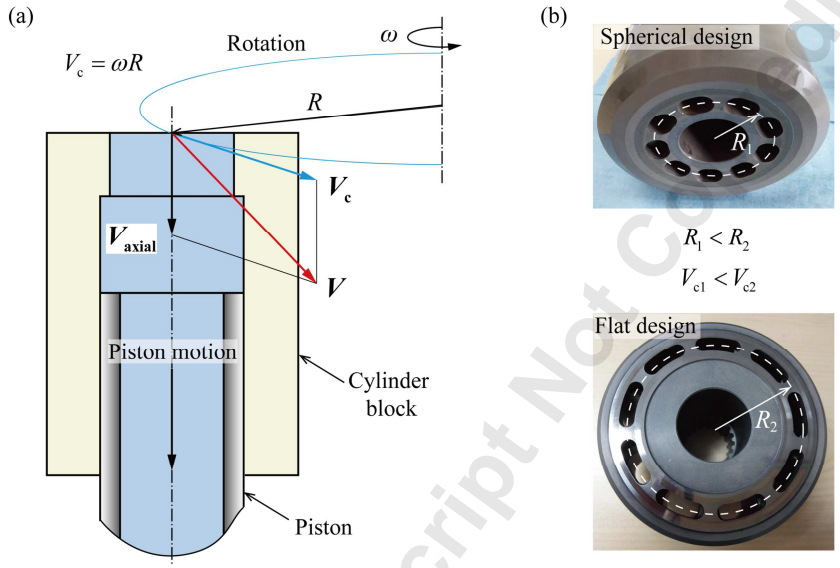

Fig. 7 Spherical design for the cylinder block bottom surface to reduce pressure losses: (a) velocity of the hydraulic fluids entering the cylinder chamber; (b) comparison of the circumferential velocity between the spherical and flat designs for the cylinder block bottom surface

Another effective method for preventing the cavitation is to optimize the valve plate. This method aims to reduce the reverse flow by minimizing the differential pressure between the cylinder chamber and the pump port at the start of suction and discharge strokes. The reduction of differential pressure can reduce the pressure undershoot at the start of suction stroke and the jet flow at the start of discharge stroke. There are two common ways to realize the reduction of differential pressure, i.e., optimizing the geometry of relief groove [30] and changing the timing angle of the valve plate [28,52,53]. However, the relief groove size and valve plate timing are highly dependent on the operating conditions such as delivery and suction pressures, pump displacement, and rotational speed and direction [54], which cannot satisfy the wide range of operating conditions for bi-directional EHA pumps. For instance, the optimized size and timing are suitable at low rotational speed, but they become too much restrictive at high rotational speed, resulting in large pressure undershoot and cavitation [27,55].

Other methods are also found to prevent the onset of cavitation and to reduce the cavitation damage. **Figure 8** shows a valve plate that integrates a pre-expansion volume (PEV) between the suction and discharge ports [56]. When the cylinder port arrives at the PEV they are connected to each other, enabling the fluid of the cylinder chamber to release its high-pressure energy gradually without the attendant cavitation problems. Machining a damping hole at the relief groove of the valve plate is useful to reduce the cavitation erosion. As shown in Fig. **9**, the damping hole increases the jet angle and thereby makes the cavitation collapse away from the solid surface of the valve plate [33]. However, the generated vapor bubbles and jetting flow in the damping hole can cause erosion damage there [57]. In addition, increasing the number of relief grooves [31] and integrating a resonator [48] are two possible ways to reduce the cavitation of the pump.

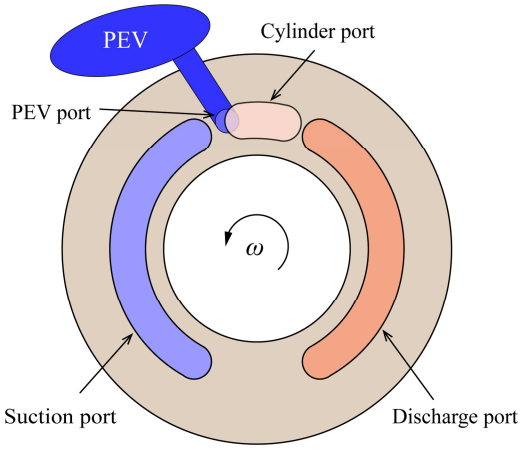

Fig. 8 Schematic of the pre-expansion volume (PEV) [56]

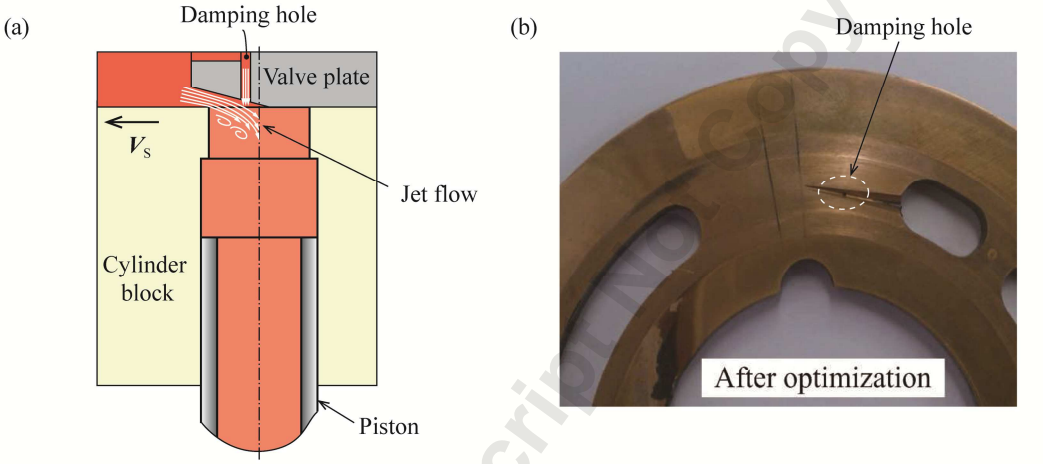

Fig. 9 Valve plate with damping hole at the relief groove: (a) effect of the damping hole on the jet flow; (b) photograph of the valve plate with damping hole after a 1000 h endurance test [33]

3. Flow and pressure ripples

The delivery flow ripple of axial piston pumps comes from two sources: (1) the kinematic flow ripple due to the finite number of pistons; (2) the dynamic flow ripple due to the reverse flow from the discharge port to the cylinder chambers at the start of the discharge stroke. The studies [27,58,59] have suggested that the major component of the delivery flow ripple results from the short-duration reverse flow rather than the finite number of pistons. The delivery flow ripple interacts with the hydraulic circuit in a complicated manner and creates corresponding pressure ripple [60]. Similarly, the flow and pressure ripples arise during suction stroke [61,62].

Many theoretical and experimental studies [63–66] have confirmed that the flow and pressure ripples increase with the pump speed. As previously stated, the reverse flow increases with the pump speed. On the other side, the relief groove may become too restrictive at high speed, leading to large cylinder pressure overshoot and undershoot. These two contributors tend to increase the flow and pressure ripples. Therefore, flow and pressure ripples are another challenge for high-speed EHA pumps. The generated pressure ripple is propagated through the flowing fluid, causing vibration of involved components and air-borne noise [64,67,68]. At the same time, the pressure ripple can lead to fatigue failure of system components and has adverse effects on the overall reliability of hydraulic systems.

To reduce the flow and pressure ripples and the consequent air-borne noise, attempts have been made over the last several decades. The valve plate is a key component to determine the level of flow and pressure ripples because a great noise reduction can be achieved through small modifications of the valve plate. The optimization of the valve plate is mainly focused on the relief groove size and timing angle of the valve plate [69–73], enabling a perfect match of pressure

between the cylinder chamber and the suction and discharge ports. In addition, the damping hole [74] of the valve plate can also reduce the flow ripple by pre-pressurizing and pre-depressurizing the cylinder fluid before the cylinder port communicates with the discharge and suction ports, respectively. However, the above solutions suffer from the drawbacks of high sensitivity to the operating conditions. Specifically, these geometrically fixed methods are effective only for particular operating points, but no longer have the optimal performance in flow ripple reduction for other operating points. In addition, the pre-compression relief groove can decrease the volumetric efficiency of the pump when there exists a cross porting between suction and discharge ports [75,76]. Although the adjustable valve plate geometry and variable valve plate timing have been reported to reduce the flow ripple at all operating points [77], they are rather complex and need to be electronically activated to offer full flexibility [78].

The cross angle (also called secondary angle) [79–83] is considered to be a promising design feature for the reduction of flow ripple and noise because it allows a varying cylinder pre-compression and decompression with the swash-plate angle by advancing or delaying the dead centers. As shown in **Fig. 10**, the cross angle describes a fixed small angle by tilting the swash plate around the axis perpendicular to the pivoting axis of the swash plate. Compared with the method of cross angle, the combination of cross angle and relief groove [84] has a greater potential to extend the operating conditions of low flow ripples.

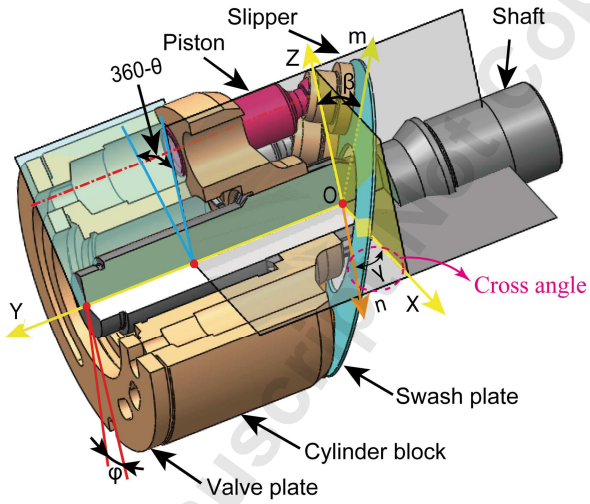

Fig. 10 Cross angle in an axial piston pump [84]

The pre-compression filter volume (PCFV) [59,85–87] can also decrease the flow ripple by reducing the reverse flow from the discharge port to the cylinder chamber. It is an additional small volume behind the valve plate, which provides pressurized fluid to the cylinder chamber when the cylinder port passes the bottom dead center (BDC). Although the PCFV is less sensitive to the operating conditions, the above pre-compression process becomes difficult at high speed because of the inertia effect of fluid between the PCFV and cylinder chamber. In addition, compared to other methods such as relief groove and ideal timing of the valve plate, the PCFV method cannot guarantee a gradual pre-compression. This will cause an increased amplitude of the swash plate moment and thus a higher structure-borne noise level [88]. The drawbacks of the PCFV can be overcome by combining the control valve and the pre-compression volume [78].

The check valve [59,86] (see **Fig. 11a**) is located ahead of the delayed discharge port and opens to the cylinder port once the cylinder pressure achieves the discharge pressure. This ideal pre-compression device can avoid pressure peaks, but in practice it has disadvantages of wear of the valve seat, conflict between stability and dynamic performance at high speed, and noise of valve itself due to undamped oscillations [78]. As an improved version of the simple check valve, the highly dynamic control valve [78] (see **Fig. 11b**) has an active and fast response to the varying operating conditions because it allows for a continuously variable flow area between the cylinder chamber and either the suction or discharge ports. To avoid the noise of the simple check valve, another modified check valve called heavily damped check valve (HDCV) [89] (see **Fig. 11c**) is designed to prevent the rapid switching action through an in-built damping system consisting of poppet, spring chamber and damping orifice. Other types of the check valves are also designed for active control of noise reduction, such as valve controlled pre-compression volume and pressure recuperation volume [78].

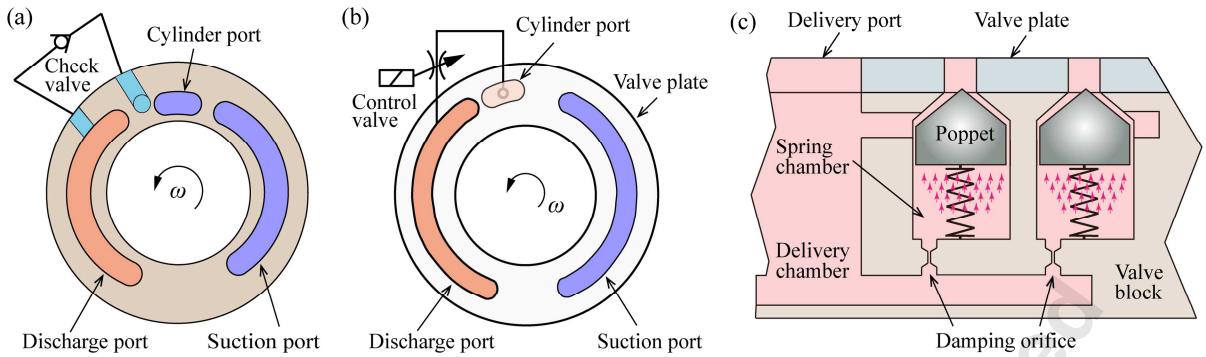

Fig. 11 Schematic of three types of check valves: (a) simple check valve [59]; (b) highly dynamic control valve [78]; (c) heavily damped check valve (HDCV) [89]

In addition, novel pulsation attenuators [90–92] for aviation pumps are also designed based on different principles. **Figure 12** shows a typical in-built pulsation attenuator which is small enough to be integrated into the aviation pump [93]. This pulsation attenuator enables the aviation pump to reduce its pressure ripple below ± 1% and this type of aviation pump has been successfully applied to aircraft A380.

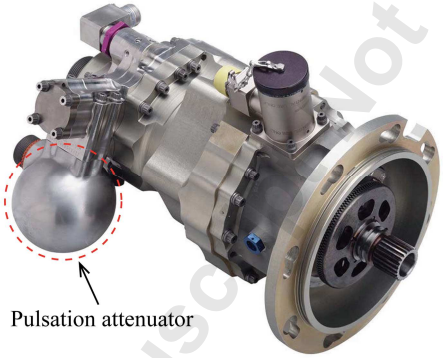

Fig. 12 The in-built pulsation attenuator in an aviation pump [93]

4. Tilting motion of rotating group

The design of the rotating group in axial piston machines is the key to the design of the pump. A typical rotating group is comprised of a valve plate, a cylinder block, multiple pistons and slippers, a swash plate and a retaining mechanism. The lubricating interfaces represent the most critical design issue for the rotating group. There are three main lubricating interfaces formed inside the rotating group, i.e., slipper/swash plate interface, piston/cylinder block interface and cylinder block/valve plate interface. These three lubricating interfaces need to fulfill the sealing and bearing functions and represent the main source of power losses [94]. Reasonable gap heights across the lubricating interfaces are essential for high efficiency and long service life of EHA pumps. Too large gap heights could increase pump leakage and decrease pump efficiency significantly. In contrast, too small gap heights could interrupt the fluid film and cause metal-to-metal contact between sliding surfaces, which can lead to seizure and/or adhesive wear and even catastrophic pump failures.

The lubrication characteristics of the interfaces are affected by the micro motions of movable parts of the rotating group. These micro motions include tilting motion, squeezing motion, and spinning motion [95], which enable the slipper, cylinder block and piston to behave as a load adaptive bearing and respond to varying external loads [96]. However, large tilting motion due to the inertial effects may become a serious problem for the rotating group at high speed [97]. It will cause a seriously asymmetrical pressure distribution and consequently reduces the load-carrying capacity of the lubricating interfaces. In addition, excessive tilting motion will produce undesirable wedge-shaped fluid film across the lubricating interfaces, leading to an increased leakage rate and potential metal-to-metal contact between movable parts of the rotating group.

For the slipper it tends to tilt away from the stationary swash plate when it rotates together with the cylinder block at high speed. The resulting tilting motion of the slipper originates from a number of tilting moments acting on it [98,99]. The first tilting moment is the centrifugal moment considering the mass center of the slipper does not generally coincide with the center of the piston-slipper ball joint. The second tilting moment arises from the viscous friction between the slipper and swash plate. The third tilting moment comes from the friction force of the piston-slipper ball joint. Among these three tilting moments, the first two moments principally result from the pump rotation and their magnitudes increase with the pump speed.

Theoretical and experimental results [98,100,101] show that the slipper is heavily tilted towards its inner edge at high speed due to the centrifugal moment acting on it. The centrifugal effect causes a more serious tilting motion of the slipper at high speed during suction stroke than during discharge stroke. This can be explained by the fact that the gap height of the slipper bearing becomes larger due to the reduced clamping force when the slipper passes from the discharge side to the suction side [102,103]. Therefore, the slipper becomes more sensitive to the centrifugal moment and is easier to tilt away from the swash plate during suction phase [104,105].

Different approaches have been used in practical applications to avoid serious slipper tilt at high speed, such as reducing the distance between the mass center of the slipper and the ball-joint center, providing sufficient inlet pressure and retaining force, and using lightweight pistons [21,104,106]. The centrifugal tilting moment acting on the slipper increases with the increasing distance between the mass center of the slipper and the ball-joint center. In contrast to the standard "female" slipper, the "male" slipper puts the ball on itself instead of on the piston, as shown in **Fig. 13**. This alternative design has the benefit of bringing the slipper's mass center nearer to the ball-joint center, thus reducing the centrifugal tilting moment acting on the slipper [107].

Fig. 13 Comparison between standard and "male" slippers: (a) standard "female" slipper; (b) "male" slipper

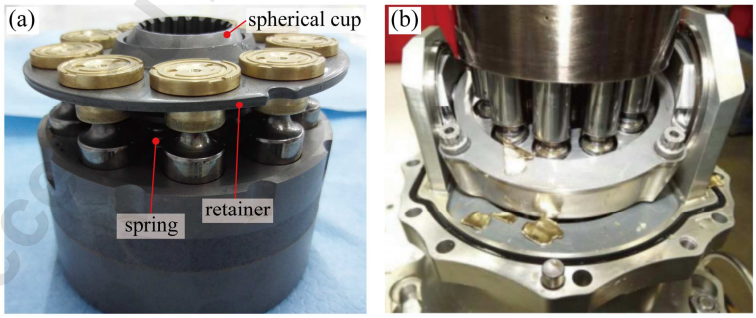

Fig. 14 Comparison between positive-force and fixed-clearance retaining mechanisms: (a) positive-force retaining mechanism; (b) fixed-clearance retaining mechanism

The slippers become very sensitive to the tilting moments when they separate from the swash plate at high speed due to the reciprocating inertia of the piston-slipper assemblies. Boosting the inlet pressure and increasing the spring load of the retaining mechanism can help the slippers to keep a reasonable contact with the swash plate at high speed. In addition, using a fixed-clearance retaining mechanism instead of a positive-force retaining mechanism can also improve the

resistance of the slippers to the reciprocating inertia of the piston-slipper assemblies. **Figure 14** shows two different types of retaining mechanisms for the slippers: positive-force retaining mechanism and fixed-clearance retaining mechanism [104,108,109]. The positive-force retaining mechanism exerts a continual preloaded spring force on the slippers by the spring, spherical cup and retainer. The fixed-clearance retaining mechanism allows for a limited clearance between the slippers and swash plate and only applies a hold-down force on the slippers when they try to pull away from the swash plate. In aerospace applications, the fixed-clearance retaining mechanism is more frequently used than the positive-force retaining mechanism because the former retaining mechanism is more reliable to prevent the slippers from tilting away from the swash plate, especially under high-speed conditions. However, the sophisticated fixed-clearance retaining mechanism requires a precise mounting and small tolerance [110].

The resistance of the slippers to the inertial effects can also benefit from using lightweight pistons. **Figure 15** shows three typical designs to reduce the piston mass [111]. The hollow piston (see **Fig. 15a**) has a cylindrical cavity which will be filled with hydraulic fluids during machine operation. This design is the cheapest and simplest to manufacture, but it creates a large void dead volume within the piston chamber that needs to be compressed and decompressed as the piston makes a transition from the suction port to discharge port and vice versa. This additional fluid compression not only reduces the efficiency of the pump, but also increases the reverse flow [58]. To reduce the void dead volume of pistons, the capped or filled pistons are suggested to be used. The capped piston (see **Fig. 15b**) maintains air within the inner core of the piston and has a small damping hole to communicate hydraulic fluids between the cylinder chamber and slipper pocket. As an alternative to the capped piston, the filled piston (see **Fig. 15c**) uses a lightweight material to fill the inner core of the piston. Although filled or capped pistons show a good compromise between piston weight and void dead volume within the piston chamber, the issues of manufacturing cost, strength, and reliability for these two pistons must be considered in practical applications.

Besides, other methods for improving the anti-tilting ability and wear resistance of the slipper include geometry optimization of the slipper [112], coating on the slipper surface [113–116] , and new materials for the slipper pair.

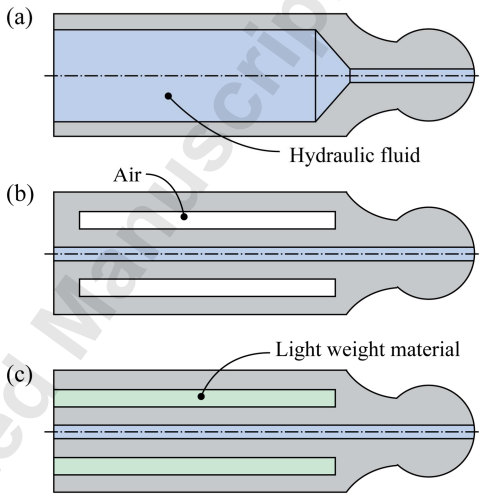

Fig. 15 Comparison between three types of pistons [111]: (a) hollow piston; (b) capped piston; (c) filled piston

Similarly, the cylinder block tends to tilt away from the stationary valve plate at high speed due to the centrifugal effect of the piston-slipper assemblies. As shown in **Fig. 16**, the centrifugal forces exerted on the multiple piston-slipper assemblies are transmitted to the cylinder block, leading to a tilting moment acting on the cylinder block [21,110,117]. To some extent, the connection of the cylinder block and the shaft via a spline mechanism allows the cylinder block to move in the z-direction and rotate around the x- and y-axis on a micro scale in addition to the macro rotation about the z-axis [118–120]. Under high-speed conditions the considerable centrifugal moment of the piston-slipper assemblies causes the cylinder block to be heavily tilted towards the BDC on the valve plate [11]. The serious tilting motion of the cylinder block results in wedge-shaped fluid film across the cylinder block/valve plate interface, increasing the leakage as well as the possibility of the metallic contact between the cylinder block and valve plate. Furthermore, the metallic contact can cause abrasion of the valve plate, which leads to vibration when the cylinder block passes the worn area of the valve plate

periodically [121].

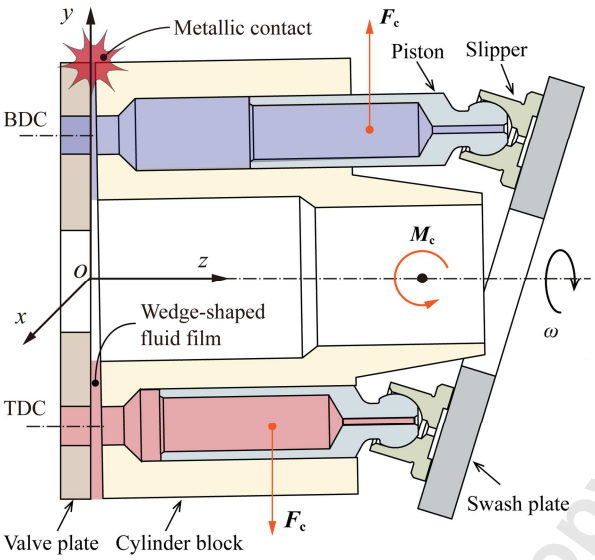

Fig. 16 Tilting motion of the cylinder block due to the centrifugal effect

Measures can be taken to avoid the cylinder block tilt or to reduce its detrimental effects. It is clear that reducing the centrifugal tilting moment acting on the cylinder block can help to decrease the cylinder block tilt at high speed. On one side, the centrifugal tilting moment can be reduced by using lightweight pistons (see **Fig. 15**). On the other side, the inverted design with a female piston and a male slipper (see **Fig. 13b**) can also reduce the centrifugal tilting moment because this specific design decreases the overhang length of the piston that represents the moment arm [110,122,123].

In addition, theoretical and experimental studies [124,125] have shown that the centrifugal tilting moment acting on the cylinder block is sensitive to the manufacturing errors of the rotating group. Only small manufacturing errors can produce significant additional centrifugal tilting moment acting on the cylinder block at high speed. Therefore, strict manufacturing tolerance of the rotating group must be achievable for high-speed EHA pumps to make the centrifugal tilting moment as small as possible.

Once the cylinder block tends to tilt away from the valve plate, the preloaded spring force acting on the cylinder block should be sufficient to push the cylinder block against the valve plate, especially at high speed and low discharge pressure. The required spring force increases with the square of the pump speed, and the spring force is generally chosen for the highest pump speed [117]. However, the EHA pump usually operates over a wide range of rotational speeds (for example, ranging from 1,000 r/min to 10,000 r/min), and the final spring force that is chosen based on the highest rotating speed will become too large when the pump operates at low rotational speed.

For an axial piston pump with its shaft going through the entire length of the machine (see **Fig. 1b**), the cylinder block spline needs to extend far enough to support the rotating group at high speed [126]. Otherwise, the tilting moments acting on the cylinder block cannot be completely counteracted by the reaction of the cylinder block spline, which can cause the cylinder block to be heavily tilted relative to the valve plate. On the other hand, a long cylinder block spline is accompanied by an increased risk of jamming between the cylinder block and shaft. This problem could be avoided by using a spherical or barrel-shaped splined shaft to match the extended cylinder block spline [99].

Decreasing the deflection of the shaft can reduce the tilting angle between the cylinder block and valve plate, which is beneficial to reduce the possibility of metallic contact between the cylinder block and valve plate. There are two approaches to reduce the deflection of the shaft. The first is to increase the rigidity of the shaft and pump casing [127,128]. The second is to install a bearing at the outer circumference of the cylinder block [99]. In this case, the bending moments acting on the cylinder block are counteracted by the bearing rather than the shaft. This design is advantageous for small-displacement EHA pumps because enough installation space and acceptable linear velocity can be achieved for the bearing.

Finally, using a spherical valve plate instead of a flat one can improve the robustness of the cylinder block to the tilting motion at high speed [49–51,129,130]. In the case of flat valve plate and cylinder block, a metal-to-metal contact will

first take place on the outer circumferences of both parts if the cylinder block tends to tilt away from the valve plate. In contrast, in the case of spherical valve plate and cylinder block, the cylinder block can slide against the valve plate accordingly. This micro degree-of-freedom enables the cylinder block to dynamically adjust its attitude relative to the valve plate, avoiding metallic contact between the cylinder block and valve plate.

5. Heat problem

The combination of small displacement and high rotational speed will increase the heat dissipation and decrease the cooling capacity of EHA pumps [131,132]. Moreover, for the self-contained and localized EHA system, the heat generated by the electric motor and EHA pump cannot be carried away by hydraulic fluids due to the elimination of centralized hydraulic systems. Instead, the heated EHA can only be cooled in the form of conduction [133–136]. As a result, a large amount of heat is left inside the EHA pump, raising concerns about the heat problem for the pump design.

As for the pump itself, the heat generation comes from leakage loss and mechanical loss [137]. As previously states, the lubricating interfaces are the primary source of power losses in axial piston machines. The movable parts of the rotating group tend to tilt at high speed and thus the wedge-shaped fluid films are formed across the lubricating interfaces, leading to an increased leakage flow and potential metal-to-metal contact. Also, the combining effect of high-speed and high-pressure conditions creates a great PV value for the lubricating interfaces, which is also identified as a main contributor to the mechanical loss [138]. In addition, the churning loss that results from the drag of the rotating group in the fluid-filled pump casing is another critical mechanical dissipation at high speed. [139,140]. Experimental and numerical studies [141–144] show that the churning loss cannot be neglected at the prevailing operating conditions, especially at high speed and low pressure.

The large amount of heat has adverse effects on the lubricating interfaces and eventually influences the lifetime of the pump. Firstly, the generated heat reduces the viscosity of hydraulic fluids, leading to an increased leakage from the lubricating interfaces. Also, viscosity reduction of hydraulic fluids tends to deteriorate the load-carrying capacity of the lubricating interfaces, which may cause severe wear and seizure of the sliding surfaces [145,146]. Secondly, the cavitation is more likely to occur at lower viscosity because the localized low pressure caused by vortices is more difficult to suppress [147]. Thirdly, the generated heat is transferred to the rotating parts and their stationary counterparts, and in turn affects the fluid film in the following two ways [139]. The temperature distribution of the solid parts determines the major boundary conditions of the non-isothermal fluid flow, and the thermal deformation of the solid parts changes the fluid film thickness in the lubricating interfaces.

To accurately predict the energy losses and heat generation of the pump, fluid-structure-thermal interaction models have been developed for the slipper/swash plate interface [109,123,148], piston/cylinder block interface [149,150], and cylinder block/valve plate interface [50,51,151,152]. Based on these models, some novel designs are proposed to reduce the energy losses and heat generation of these lubricating interfaces. For example, micro surface shapes are used on the movable parts and their stationary counterparts, such as waved, contoured or barreled pistons [153–159], concave cylinder bore [160], waved valve plate [161–163], and surface texturing for tribological interfaces [164–168]. These micro surface shapes can produce an additional micro-hydrodynamic pressure in the lubricating interfaces, thus improving the load-carrying capacity of the fluid film. This helps to avoid metal-to-metal contact between components under extreme conditions and to reduce attendant heat generation.

In recent years, the surface coating technology has been tried on the slippers [113–116] and pistons [169–174] of axial piston pumps to improve their wear resistance and to reduce their friction coefficient, thus reducing the heat dissipation caused by metallic contact. Furthermore, removal of certain lubricating interfaces can offer a potential solution to the reduction of heat dissipation. For instance, the slipper/swash plate interface is absent in both bent-axis type piston pumps and floating cup pumps compared to swash-plate type axial piston pumps [118].

Finally, the reduction of heat generation can benefit from reducing the churning loss of the rotating group. Compared with the conventional fluid-filled pump casing, the dry pump casing has great potential for low churning loss [175]. However, the dry pump casing significantly reduces the cooling capacity of the pump due to the removal of hydraulic fluids, even worsening the overheating problem. It is possible to install a “power boost insert” into the pump casing to prevent the hydraulic fluids from moving around in a turbulent manner [176], as shown in **Fig. 17.** The experimental results show that the pump with an insert has a 3% higher efficiency than a standard pump. Nano-coating on the cylinder

block is another effective way to decrease the churning loss by providing a low roughness and wettability [177] for the cylinder block surface.

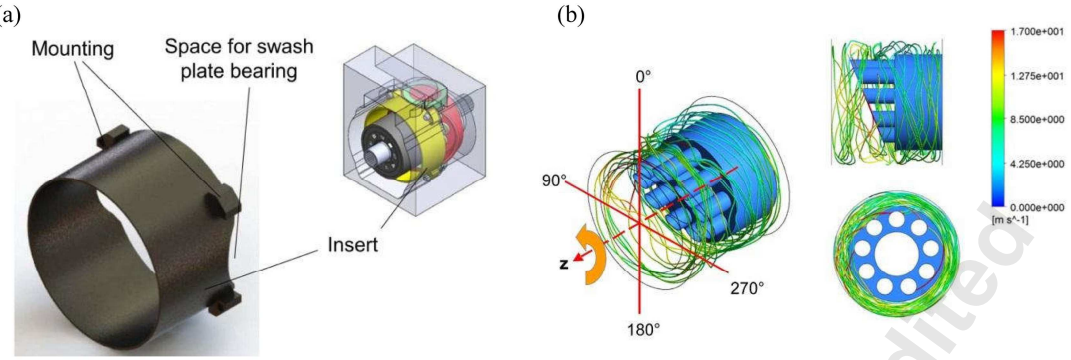

Fig. 17 Insert in the pump casing to reduce churning loss [176]: (a) configuration of an insert; (b) effect of the insert on the turbulent flow in a pump casing

6. Conclusions

This review highlights the challenges of high-speed rotation for EHA pumps and details possible solutions. These challenges include the cavitation, flow and pressure ripples, tilting motion of rotating group, and heat problem. Among the presented solutions, some of them have been successfully applied to commercial pump products, such as spherical valve plate, "male" slipper, fixed-clearance retaining mechanism, capped piston, and pulsation attenuator. Some solutions have been used in other similar hydraulic products but have not been applied to axial piston pumps. For example, the insert has been used in the high-speed bent-axis type piston motors delivered by Parker. Although some new solutions are still in study, they appear promising for EHA pumps. For example, the advanced technologies of micro-surface shaping and surface coating could be applied to EHA pump products if the mature and low-cost technological processes are available in the future.

In addition to the challenges and solutions discussed in this review, the following issues are also recommended in the future research on EHA pumps: (1) new materials with good resistance to wear and cavitation erosion for low-viscosity hydraulic fluid; (2) advanced lubrication technology with low friction coefficient and wear rate; (3) temperature prediction and control for small size pumps; (4) nonlinear rotor dynamics of the rotating group submerged in hydraulic fluids.

Conflict of interest

The authors declare that they have no conflict of interest.

Funding

This study was supported by the National Natural Science Foundation of China [Grant No. U1737110], the National Basic Research Program of China (973 Program) [Grant No. 2014CB046403], and the National Natural Science Foundation of China [Grant No. 51605425].

Nomenclature

$\boldsymbol{F}_c$ = centrifugal force of the piston-slipper assembly
h = relief groove opening of the valve plate
$\boldsymbol{M}_c$ = tilting moment acting on the cylinder block by the centrifugal force $\boldsymbol{F}_c$
n = rotational speed of the pump
n_{Lim} = rotational speed limit
n_{nom} = rated rotational speed limit

p_1 = discharge pressure
$p_{1,nom}$ = rated maximum discharge pressure
p_s = suction pressure
$p_{s,nom}$ = rated suction pressure
Q_1 = delivery flow rate
$Q_{1,nom}$ = theoretic delivery flow rate at n_{nom}
R = pitch radius of the cylinder ports
R_1 = pitch radius of the cylinder ports for the spherical cylinder block
R_2 = pitch radius of the cylinder ports for the flat cylinder block
$\boldsymbol{V}$ = resultant velocity of the hydraulic fluids entering the cylinder chamber
V_1 = pump displacement
$V_{1,max}$ = maximum pump displacement
$\boldsymbol{V}_{\mathbf{axial}}$ = axial component of the resultant velocity $\boldsymbol{V}$
$\boldsymbol{V}_{\mathbf{c}}$ = circumferential component of the resultant velocity $\boldsymbol{V}$
$\boldsymbol{V}_{\mathbf{c1}}$ = circumferential velocity component for the spherical cylinder block
$\boldsymbol{V}_{\mathbf{c2}}$ = circumferential velocity component for the flat cylinder block
$\boldsymbol{V}_{\mathbf{S}}$ = sliding velocity of the cylinder block relative to the valve plate
α_0 = dissolved air volume fraction
α_s = Bunsen coefficient
β = swash-plate angle
γ = cross angle
θ = angular displacement of the cylinder block
φ = timing angle of the valve plate
ω = rotational speed of the cylinder block

Abbreviations

BDC = bottom dead center
EHA = electro-hydrostatic actuator
HDCV = heavily damped check valve
HP = high pressure
LP = low pressure
PBW = power by wire
PCFV = pre-compression filter volume
PEV = pre-expansion volume
TDC = top dead center

References

[1] Van Den Bossche, D., 2006, "The A380 flight control electrohydrostatic actuators, achievements and lessons learnt," 25th International Congress of The Aeronautical Sciences, Hamburg, Germany.
[2] Alle, N., Hiremath, S. S., Makaram, S., Subramaniam, K., and Talukdar, A., 2016, "Review on electro hydrostatic actuator for flight control," Int. J. Fluid Power, **17**(2), pp. 125–145.
[3] Chakraborty, I., Mavris, D. N., Emeneth, M., and Schneegans, A., 2015, "A methodology for vehicle and mission level comparison of more electric aircraft subsystem solutions: application to the flight control actuation system," Proc. Inst. Mech. Eng. Part G: J. Aerosp. Eng., **229**(6), pp. 1088–1102.
[4] Navarro, R., 1997, "Performance of an electro-hydrostatic actuator on the F-18 systems research aircraft," Technical Report No. NASA/TM-97–206224, Dryden Flight Research Center, NASA.
[5] Wiegand, C., Bullick, B. A., Catt, J. A., Hamstra, J. W., Walker, G. P., and Wurth, S., 2018, "F-35 air vehicle technology

overview," 2018 Aviation Technology, Integration, and Operations Conference, Atlanta, USA.
[6] Robbins, D., Bobalik, J., De Stena, D., Martin, N., Plag, K., Rail, K., and Wall, K., 2018, "F-35 subsystems design, development & verification," 2018 Aviation Technology, Integration, and Operations Conference, Atlanta, USA.
[7] Maré, J. C., and Fu, J., 2017, "Review on signal-by-wire and power-by-wire actuation for more electric aircraft," Chin. J. Aeronaut., **30**(3), pp. 857–870.
[8] Botten, S. L., Whitley C. R., and King A. D., 2000, "Flight control actuation technology for next-generation all-electric aircraft the benefits of electric actuation," Technol. Rev. J., **8**(2), pp. 55–68.
[9] Roboam, X., Sareni, B., and De Andrade, A., 2012, "More electricity in the air: Toward optimized electrical networks embedded in more-electrical aircraft," IEEE Ind. Electron. Mag., **6**(4), pp. 6–17.
[10] Habibi, S., 2000, "Design of a new high-performance electrohydraulic actuator," IEEE-ASME Trans. Mechatron., **5**(2), pp. 158–164.
[11] Zhang, J. H., Chao, Q., and Xu, B., "Analysis of the cylinder block tilting inertia moment and its effect on the performance of high-speed electro-hydrostatic actuator pumps of aircraft," Chin. J. Aeronaut., **31**(1), pp. 169–177.
[12] Wu, S., Yu, B., Jiao, Z. X., Shang, Y. X., and Luk, P., 2017, "Preliminary design and multi-objective optimization of electro-hydrostatic actuator," Proc. Inst. Mech. Eng. Part G: J. Aerosp. Eng., **231**(7), pp. 1258–1268.
[13] Crowder, R. M., 1996, "Electrically powered actuation for civil aircraft," IEE Colloquium on Actuator Technology: Current Practice and New Developments (Digest No: 1996/110), London, UK.
[14] Totten, G. E., Sun, Y. H., Bishop, R. J., and Lin, X., 1998, "Hydraulic system cavitation: A review," SAE Technical Paper No. 982036.
[15] Schleihs, C., Viennet, E., Deeken, M., Ding, H., Xia, Y. J., Lowry, S., and Murrenhoff, H., 2014, "3D-CFD simulation of an axial piston displacement unit," 9th International Fluid Power Conference, Aachen, Germany.
[16] Lyer, C. O., and Yang, W. J., 1999, "Analysis on liquid-vapor bubbly-flow systems in reciprocating motion," ASME J. Fluids Eng., **121**(1), pp. 185–190.
[17] Bishop, R. J., and Totten, G. E., 2001, "Effect of pump inlet conditions on hydraulic pump cavitation: A review," Hydraulic Failure Analysis: Fluids, Components, and System Effects, ASTM International.
[18] Totten, G. E., and Bishop, R. J., 1999, "The hydraulic pump inlet condition: impact on hydraulic pump cavitation potential," SAE Technical Paper No. 1999-01-1877.
[19] Hibi, A., Ibuki, T., Ichikawa, T., and Yokote, H., 1977, "Suction performance of axial piston pump: 1st report, analysis and fundamental experiments," Bull. JSME, **20**(139), pp. 79–84.
[20] Ibuki, T., Hibi, A., Ichikawa, T., and Yokote, H., 1977, "Suction performance of axial piston pump: 2nd report, experimental results," Bull. JSME, **20**(145), pp. 827–833.
[21] Manring, N. D., Mehta, V. S., Nelson, B. E., Graf, K. J., and Kuehn, J. L., 2014, "Scaling the speed limitations for axial-piston swash-plate type hydrostatic machines," ASME J. Dyn. Syst. Meas. Control, 136(3), p. 031004.
[22] Totten, G. E., Sun, Y. H., and Bishop, R. J., 1999, "Hydraulic system cavitation: Part II–a review of hardware design–related effects," SAE Technical Paper No. 1999-01-2857.
[23] Saxena, D., 2008, "CFD modeling of cavitation in an axial piston pump," M.S. Thesis, Purdue University, USA.
[24] Harris, R. M., Edge, K. A., and Tilley, D. G., 1994, "The suction dynamics of positive displacement axial piston pumps," ASME J. Dyn. Syst. Meas. Control, **116**(2), pp. 281–287.
[25] Edge, K. A., and Darling, J., 1986, "Cylinder pressure transients in oil hydraulic pumps with sliding plate valves," Proc. Inst. Mech. Eng. Part B: J. Eng. Manuf., **200**(1), pp. 45–54.
[26] Edge, K. A., and Darling, J., 1989, "The pumping dynamics of swash plate piston pumps," ASME J. Dyn. Syst. Meas. Control, **111**(2), pp. 307–312.
[27] Darling, J., 1985, "Piston-cylinder dynamics in oil hydraulic axial piston pumps" Ph.D. Thesis, University of Bath, UK.
[28] Mandal, N. P., Saha, R., and Sanyal, D., 2012, "Effects of flow inertia modelling and valve-plate geometry on swash-plate axial-piston pump performance," Inst. Mech. Eng. Part I: J. Syst. Control Eng., **226**(4), pp. 451–465.
[29] Yamaguchi, A., and Takabe, T., 1983, "Cavitation in an axial piston pump," Bull. JSME, **26**(211), pp. 72–78.
[30] Shi, Y. X., Lin, T. R., Meng, G. Y., and Huang, J. X., 2016, "A study on the suppression of cavitation flow inside an axial piston pump," Prognostics and System Health Management Conference, Chengdu, China.
[31] Tsukiji, T., Nakayama, K., Saito, K., and Yakabe, S., 2011, "Study on the cavitating flow in an oil hydraulic pump," 2011 International Conference on Fluid Power and Mechatronics, Beijing, China, pp. 253–258.
[32] Ito, K., Inoue, K., and Saito, K., 1996, "Visualization and detection of cavitation in V-shaped groove type valve plate of an axial piston pump," JFPS Int. Symp. Fluid Power, **1996**(3), pp. 67–72.
[33] Liu, W., Wang, A. L., Shan, X. W., Zhang, X. L., and Jiang, T., 2014, "Valve plate for piston pump cavitation problem with the damp groove structural optimization," Appl. Mech. Mater., **543–547**, pp. 154–157.
[34] Kunkis, M., and Weber, J., 2016, "Experimental and numerical assessment of an axial piston pump's speed limit," BATH/ASME 2016 Symposium on Fluid Power and Motion Control, Bath, UK.
[35] Vacca, A., Klop, R., and Ivantysynova, M., 2010, "A numerical approach for the evaluation of the effects of air release and vapour cavitation on effective flow rate of axial piston machines," Int. J. Fluid Power, **11**(1), pp. 33–45.

[36] Gullapalli, S., Kensler, J., Taylor, R. I., Michael, P., Cheekolu, M., and Lizarraga-Garcia, E., 2017, "An investigation of hydraulic fluid composition and aeration in an axial piston pump," ASME/BATH 2017 Symposium on Fluid Power and Motion Control, Sarasota, Florida, USA.
[37] Casoli, P., Vacca, A., Franzoni, G., and Berta, G. L., 2006, "Modelling of fluid properties in hydraulic positive displacement machines," Simul. Model Pract. Theory, **14**(8), pp. 1059–1072.
[38] Ruan, J., and Burton, R., 2006, "Bulk modulus of air content oil in a hydraulic cylinder," ASME International Mechanical Engineering Congress and Exposition, Chicago, Illinois, USA.
[39] Gholizadeh, H., Burton, R., and Schoenau, G., 2012, "Fluid bulk modulus: Comparison of low pressure models," Int. J. Fluid Power, **13**(1), pp. 7–16.
[40] Schrank, K., Murrenhoff, H., and Stammen, C., 2013, "Measurements of air absorption and air release characteristics in hydraulic oils at low pressure," ASME/BATH 2013 Symposium on Fluid Power and Motion Control, Sarasota, Florida, USA.
[41] Fey, C. G., Totten, G. E., Bishop, R. J., and Ashraf, A., 2000, "Analysis of common failure modes of axial piston pumps," SAE Technical Paper No. 2000-01-2581.
[42] Ding, H., Visser, F. C., Jiang, Y., and Furmanczyk, M., 2011, "Demonstration and validation of a 3D CFD simulation tool predicting pump performance and cavitation for industrial applications," ASME J. Fluids Eng., **133**(1), p. 011101.
[43] Yin, F. L., Nie, S. L., Xiao, S. H., and Hou, W., 2016, "Numerical and experimental study of cavitation performance in sea water," Proc. Inst. Mech. Eng. Part I: J. Syst. Control Eng., **230**(8), pp. 716–735.
[44] "Engine-driven pump model PV3-240-18", 2013, Available: www.eaton.com/Eaton/ProductsServices/Aerospace/LiteratureLibrary/index.htm?litlibtarget=979679288156.
[45] Edge, K. A., and de Freitas, F. J. T., 1985, "A study of pressure fluctuations in the suction lines of positive displacement pumps," Proc. Inst. Mech. Eng. Part B: J. Eng. Manuf., **199**(4), pp. 211–217.
[46] Mohn, G., and Nafz, T., 2016, "Swash plate pumps–the key to the future," 10th International Fluid Power Conference, Dresden, Germany, pp. 139–150.
[47] Bügener, N., Klecker, J., and Weber, J., 2014, "Analysis and improvement of the suction performance of axial piston pumps in swash plate design," Int. J. Fluid Power, **15**(3), pp. 153–167.
[48] Bügener, N., and Helduser, S., 2010, "Analysis of the suction performance of axial piston pumps by means of computational fluid dynamics (CFD)," 7th International Fluid Power Conference, Aachen, Germany.
[49] Kosodo, H., 2012, "Development of micro pump and micro-HST for hydraulics," JFPS Int. J. Fluid Power Syst., **5**(1), pp. 6–10.
[50] Zecchi, M., and Ivantysynova, M., 2013, "Spherical valve plate design in axial piston machines–A novel thermoelasto-hydrodynamic model to predict the lubricating interface performance," 8th International Conference on Fluid Power Transmission and Control, Hangzhou, China, pp. 325–329.
[51] Zecchi, M., 2013, "A novel fluid structure interaction and thermal model to predict the cylinder block/valve plate interface performance in swash plate type axial piston machines," Ph.D. Thesis, Purdue University, USA.
[52] Berta, G. L., Casoli, P., Vacca, A., and Guidetti, M., 2002, "Simulation model of an axial piston pump inclusive of cavitation," ASME International Mechanical Engineering Congress and Exposition, New Orleans, Louisiana, USA.
[53] Wang, S., 2010, "The analysis of cavitation problems in the axial piston pump," ASME J. Fluids Eng., **132**(7), p. 074502.
[54] Martin, M. J., and Taylor, R., 1978, "Optimised port plate timing for an axial piston pump," 5th International Fluid Power Symposium, Durham, England, Paper B5, pp. 51–66.
[55] Helgestad, B. O., Foster, K., and Bannister, F. K., 1974, "Pressure transients in an axial piston hydraulic pump," Proc. Inst. Mech. Eng., **188**(1), pp. 189–199.
[56] Harris, R. M., Edge, K. A., and Tilley, D. G., 1992, "Reduction of piston pump cavitation by means of a pre-expansion volume," 5th Bath International Fluid Power Workshop, Bath, UK, pp. 167–183.
[57] Ye, S. G., Zhang, J. H., Xu, B., Song, W., Chen, L., Shi, H. Y., and Zhu, S. Q., 2017, "Experimental and numerical studies on erosion damage in damping holes on the valve plate of an axial piston pump," J. Mech. Sci. Technol., **31**(9), pp. 4285–4295.
[58] Manring, N. D., 2000, "The discharge flow ripple of an axial-piston swash-plate type hydrostatic pump," ASME J. Dyn. Syst. Meas. Control, **122**(2), pp. 263–268.
[59] Pettersson, M. E., Weddfelt, K. G., and Palmberg, J. S., 1991, "Methods of reducing flow ripple from fluid power pumps-a theoretical approach," SAE Technical Paper No. 911762.
[60] Edge, K. A., and Wing, T. J., 1983, "The measurement of the fluid borne pressure ripple characteristics of hydraulic components," Proc. Inst. Mech. Eng. Part B: J. Eng. Manuf., **197**(4), pp. 247–254.
[61] Edge, K. A., and Freitas, F., 1981, "Fluid borne pressure ripple in positive displacement pumps suction lines," 6th International Fluid Power Symposium, Cambridge, England, Paper D4, pp. 205–217.
[62] de Freitas, F. J. T., 1982, "The generation and transmission of pressure fluctuations in pump suction lines," Ph.D. Thesis, University of Bath, UK.
[63] Edge, K. A., and Darling, J., 1988, "A theoretical model of axial piston pump flow ripple," 1st Bath International Fluid Power Workshop, Bath, England, pp. 113–136.
[64] Kim, J. K., Kim, H. E., Jung, J. Y., Oh, S. H., and Jung, S. H., 2004, "Relation between pressure variations and noise in axial type oil piston pumps," KSME Int. J., **18**(6), pp. 1019–1025.

[65] Bergada, J. M., Kumar, S., Davies, D. L., and Watton, J., 2012, "A complete analysis of axial piston pump leakage and output flow ripples," Appl. Math. Model, **36**(4), pp. 1731–1751.
[66] Xu, B., Hu, M., and Zhang, J. H., 2015, "Impact of typical steady-state conditions and transient conditions on flow ripple and its test accuracy for axial piston pump," Chin. J. Mech. Eng., **28**(5), pp. 1012–1022.
[67] Wang, Z. M., and Tan, S. K., 1998, "Vibration and pressure fluctuation in a flexible hydraulic power systemon an aircraft," Comput. Fluids, **27**(1), pp. 1–9.
[68] Ouyang, X. P., Fang, X., and Yang, H. Y., 2016, "An investigation into the swash plate vibration and pressure pulsation of piston pumps based on full fluid-structure interactions," J. Zhejiang Univ.-Sci. A, **17**(3), pp. 202–214.
[69] Song, Y. C., Xu, B., and Yang, H. Y., 2011, "Study on effect of relief groove angle expressing the position in reducing noise of swash plate axial piston pump," Adv. Mater. Res., **311–313**, pp. 2215–2224.
[70] Yin, F. L., Nie, S. L., Hou, W., and Xiao, S. H., 2017, "Effect analysis of silencing grooves on pressure and vibration characteristics of seawater axial piston pump," Proc. Inst. Mech. Eng. Part C: J. Mech. Eng. Sci., **231**(8), pp. 1390–1409.
[71] Johansson, A., and Palmberg, J. O., 2005, "The importance of suction port timing in axial piston pumps," 9th International Conference on Fluid Power, Aachen, Germany.
[72] Mandal, N. P., Saha, R., and Sanyal, D., 2008, "Theoretical simulation of ripples for different leading-side groove volumes on manifolds in fixed-displacement axial-piston pump," Inst. Mech. Eng. Part I: J. Syst. Control Eng., **222**(6), pp. 557–570.
[73] Kim, D. A., 2012, "Contribution to digital prototyping of axial piston pumps motors," M.S. Thesis, Purdue University, USA.
[74] Guan, C. B., Jiao, Z. X., and He, S. Z., 2014, "Theoretical study of flow ripple for an aviation axial-piston pump with damping holes in the valve plate," Chin. J. Aeronaut., **27**(1), pp. 169–181.
[75] Seeniraj, G. K., and Ivantysynova, M., 2006, "Impact of valve plate design on noise, volumetric efficiency and control effort in an axial piston pump," ASME International Mechanical Engineering Congress and Exposition, Chicago, Illinois, USA.
[76] Wang, S., 2012, "Improving the volumetric efficiency of the axial piston pump," ASME J. Mech. Des., **134**(11), p. 111001.
[77] Edge, K. A., and Liu, Y., 1989, "Reduction of piston pump pressure ripple," 2nd International Conference on Fluid Power Transmission and Control, Hangzhou, China, pp. 779–784.
[78] Nafz, T., Murrenhoff, H., and Rudik, R., 2008, "Active systems for noise reduction and efficiency improvement of axial piston pumps," Bath/ASME Symposium on Fluid Power and Motion Control, Bath, UK, pp. 327–340.
[79] Johansson, A., Palmberg, J. O., and Rydberg, K. E., 2001, "Cross angle—a design feature for reducing noise and vibrations in hydrostatic piston pumps," 5th International Conference on Fluid Power Transmission and Control, Hangzhou, China, pp. 62–68.
[80] Johansson, A., Andersson, J., and Palmberg, J. O., 2002, "Optimal design of the cross-angle for pulsation reduction in variable displacement pumps," Power Transmission and Motion Control, Bath, UK, pp. 319–333.
[81] Ericson, L., Ölvander, J., and Palmberg, J. O., 2007, "Flow pulsation reduction for variable displacement motors using cross-angle," Power Transmission and Motion Control, Bath, UK, pp. 103–116.
[82] Johansson, A., Ölvander, J., and Palmberg, J. O., 2007, "Experimental verification of cross-angle for noise reduction in hydraulic piston pumps," Inst. Mech. Eng. Part I: J. Syst. Control Eng., **221**(3), pp. 321–330.
[83] Wei, X. Y., and Wang, H. Y., 2012, "The influence of cross angle on the flow ripple of axial piston pumps by CFD simulation," Appl. Mech. Mater., **220–223**, pp. 1675–1678.
[84] Xu, B., Ye, S. G., Zhang, J. H., and Zhang, C. F., 2016, "Flow ripple reduction of an axial piston pump by a combination of cross-angle and pressure relief grooves: Analysis and optimization," J. Mech. Sci. Technol., **30**(6), pp. 2531–2545.
[85] Pettersson, M., Weddfelt, K., and Palmberg, J. O., 1992, "Reduction of flow ripple from fluid power machines by means of a precompression filter volume," 10th Aachen Colloquium on Fluid Power Technology, Aachen, Germany, pp. 23–47.
[86] Seeniraj, G. K., and Ivantysynova, M., 2006, "Noise reduction in axial piston machines based on multi-parameter optimization," 4th FPNI Ph.D. Symposium on Fluid Power, Sarasota, Florida, USA, pp. 235–246.
[87] Xu, B., Song, Y. C., and Yang, H. Y., 2013, "Pre-compression volume on flow ripple reduction of a piston pump," Chin. J. Mech. Eng., **26**(6), pp. 1259–1266.
[88] Ivantysynova, M., Seeniraj, G. K., and Huang, C. H., 2005, "Comparison of different valve plate designs focusing on oscillating forces and flow pulsation," 9th Scandinavian International Conference on Fluid Power, Linköping, Sweden.
[89] Harrison, A. M., and Edge, K. A., 2000, "Reduction of axial piston pump pressure ripple," Inst. Mech. Eng. Part I: J. Syst. Control Eng., **214**(1), pp. 53–64.
[90] Gao, F., Ouyang, X. P., Yang, H. Y., and Xu, X. H., 2013, "A novel pulsation attenuator for aircraft piston pump," Mechatronics, **23**(6), pp. 566–572.
[91] Waitschat, A., Thielecke, F., Behr, R. M., and Heise, U., 2016, "Active fluid borne noise reduction for aviation hydraulic pumps," 10th International Fluid Power Conference, Dresden, Germany, pp. 307–318.
[92] Li, L., Lee, K. M., Ouyang, X. P., and Yang, H. Y., 2017, "Attenuating characteristics of a multi-element buffer bottle in an aircraft piston pump," Proc. Inst. Mech. Eng. Part C: J. Mech. Eng. Sci., **231**(10), pp. 1791–1803.
[93] Hargreaves, B., 2017, "Hydraulic systems keep evolving; MRO options expand,"
Available: http://www.mro-network.com/engines-engine-systems/hydraulic-systems-keep-evolving-mro-options-expand.
[94] Wieczorek, U., and Ivantysynova, M., 2000, "Simulation of the gap flow in the sealing and bearing gaps of axial piston machines," 1st FPNI Ph.D. Symposium on Fluid Power, Hamburg, Germany, pp. 493–507.

[95] Zhang, J. H., Chao, Q., Wang, Q. N., Xu, B., Chen, Y., and Li, Y., 2017, "Experimental investigations of the slipper spin in an axial piston pump," Measurement, **102**, pp. 112–120.
[96] Schenk, A., and Ivantysynova, M., 2011, "An investigation of the impact of elastohydrodynamic deformation on power loss in the slipper swashplate interface," 8th JFPS International Symposium on Fluid Power, Okinawa, Japan, pp. 228–234.
[97] Shi, C., Wang, S. P., Wang, X. J., and Zhang, Y. X., 2018, "Variable load failure mechanism for high-speed load sensing electro-hydrostatic actuator pump of aircraft," Chin. J. Aeronaut., **31**(5), pp. 949–964.
[98] Hooke, C. J., and Li, K. Y., 1989, "The lubrication of slippers in axial piston pumps and motors—the effect of tilting couples," Proc. Inst. Mech. Eng. Part C: J. Mech. Eng. Sci., **203**(5), pp. 343–350.
[99] Ivantysyn, J., and Ivantysynova, M., 2001, "Hydrostatic pumps and motors: principles, design, performance, modelling, analysis, control and testing," Akademia Books International.
[100] Hooke, C. J., and Kakoullis, Y. P., 1981, "The Effects of centrifugal load and ball friction on the lubrication of slippers in axial piston pumps," 6th International Fluid Power Symposium, Cambridge, England, Paper D2, pp. 179–191.
[101] Harris, R. M., Edge, K. A., and Tilley, D. G., 1996, "Predicting the behavior of slipper pads in swashplate-type axial piston pumps," ASME J. Dyn. Syst. Meas. Control, **118**(1), pp. 41–47.
[102] Huang, C. C., 2004, "CASPAR based slipper performance prediction in axial piston pumps," 3rd FPNI Ph.D. Symposium on Fluid Power, Terrassa, Spain, pp. 229–238.
[103] Chao, Q., Zhang, J. H., Xu, B., and Wang, Q. N., 2018, "Multi-position measurement of oil film thickness within the slipper bearing in axial piston pumps," Measurement, **122**, pp. 66–72.
[104] Manring, N. D., 1998, "Slipper tipping within an axial-piston swash-plate type hydrostatic pump," ASME International Mechanical Engineering Congress and Exposition, Anaheim, California, USA, pp. 169–175.
[105] Borghi, M., Specchia, E., and Zardin, B., 2009, "Numerical analysis of the dynamic behaviour of axial piston pumps and motors slipper bearings," SAE Int. J. Passeng. Cars – Mech. Syst., **2**(1), pp. 1285–1302.
[106] Borghi, M., Specchia, E., Zardin, B., and Corradini, E., 2009, "The critical speed of slipper bearings in axial piston swash plate type pumps and motors," ASME 2009 Dynamic Systems and Control Conference, Hollywood, California, USA , pp. 267–274.
[107] Kakoullis, Y. P., 1979, "Slipper lubrication in axial piston pumps," Ph.D. Thesis, University of Birmingham, UK.
[108] Manring, N. D., 2001, "Designing a control and containment device for cradle-mounted, axial-actuated swash plates," ASME J. Mech. Des., **123**(3), pp. 447–455.
[109] Schenk, A., and Ivantysynova, M., 2015, "A transient thermoelastohydrodynamic lubrication model for the slipper/swashplate in axial piston machines," ASME J. Tribol., **137**(3), p. 031701.
[110] Ivantysyn, R., 2011, "Computational design of swash plate type axial piston pumps a framework for computational design," M.S. Thesis, Purdue University, USA.
[111] Manring, N. D., 2013, "Fluid power pumps and motors: analysis, design and control," McGraw-Hill Education.
[112] Xu, B., Zhang, J. H., and Yang, H. Y., 2012, "Investigation on structural optimization of anti-overturning slipper of axial piston pump," Sci. China-Technol. Sci., **55**(11), pp. 3010–3018.
[113] Lee, S. Y., Kim, S. D., and Hong, Y. S., 2005, "Application of the duplex TiN coatings to improve the tribological properties of electro hydrostatic actuator pump parts," Surf. Coat. Technol., **193** (1–3), pp. 266–271.
[114] Kalin, M., Majdič, F., Vižintin, J., Pezdirnik, J., and Velkavrh, I., 2008, "Analyses of the long-term performance and tribological behavior of an axial piston pump using diamondlike-carbon-coated piston shoes and biodegradable oil," ASME J. Tribol., **130**(1), p. 011013.
[115] Rizzo, G., Massarotti, G. P., Bonanno, A., Paoluzzi, R., Raimondom, M., Blosi, M., Veronesi, F., Caldarelli, A., and Guarini, G., 2015, "Axial piston pumps slippers with nanocoated surfaces to reduce friction," Int. J. Fluid Power, **16**(1), pp. 1–10.
[116] Rizzo, G., Bonanno, A., Massarotti, G. P., Pastorello, L., Raimondo, M., Veronesi, F., and Blosi, M., 2016, "Energy efficiency improvement by the application of nano-structured coatings on axial piston pump slippers," 10th International Fluid Power Conference, Dresden, Germany, pp. 313–328.
[117] Manring, N. D., 2000, "Tipping the cylinder block of an axial-piston swash-plate type hydrostatic machine," ASME J. Dyn. Syst. Meas. Control, **122**(1), pp. 216–221.
[118] Achten, P., and Eggenkamp, S., 2017, "Barrel tipping in axial piston pumps and motors," 15th Scandinavian International Conference on Fluid Power, Linköping, Sweden, pp. 381–391.
[119] Wegner, S., Gels, S., Jang, D. S., and Murrenhoff, H., 2015, "Experimental investigation of the cylinder block movement in an axial piston machine," ASME/BATH 2015 Symposium Fluid Power Motion Control, Chicago, Illinois, USA.
[120] Wegner, D. S., and Löschner, F., 2016, "Validation of the physical effect implementation in a simulation model for the cylinder block/valve plate contact supported by experimental investigations," 10th International Fluid Power Conference, Dresden, Germany, pp. 269–281.
[121] Du, J., Wang, S. P., and Zhang, H. Y., 2013, "Layered clustering multi-fault diagnosis for hydraulic piston pump," Mech. Syst. Signal Proc., **36**(2), pp. 487–504.
[122] Manring, N. D., Mehta, V. S., Nelson, B. E., Graf, K. J., and Kuehn, J. L., 2013, "Increasing the power density for axial-piston swash-plate type hydrostatic machines," ASME J. Mech. Des. **135**(7), p. 071002.
[123] Schenk, A. T., 2014, "Predicting lubrication performance between the slipper and swashplate in axial piston hydraulic machines,"

Ph.D. Thesis, Purdue University, USA.
[124] Xu, B., Chao, Q., Zhang, J. H., and Chen, Y., 2017, "Effects of the dimensional and geometrical errors on the cylinder block tilt of a high-speed EHA pump," Meccanica, **52**(10), pp. 2449–2469.
[125] Zhang, J. H., Chao, Q., Xu, B., Pan, M., Chen, Y., Wang, Q. N., and Li, Y., 2017, "Effect of piston-slipper assembly mass difference on the cylinder block tilt in a high-speed electro-hydrostatic actuator pump of aircraft," Int. J. Precis. Eng. Manuf., **18**(7), pp. 995–1003.
[126] Chao, Q., Zhang, J. H., Xu, B., Chen, Y., and Ge, Y. Z., 2018, "Spline design for the cylinder block within a high-speed electro-hydrostatic actuator pump of aircraft," Meccanica, **53**(1–2), pp. 395–411.
[127] Hooke, C. J., Foster, K., and Madera, G., 1975, "A note on the effect of shaft and casing stiffness on the port plate lubrication film of a particular slipper-pad axial piston pump," 4th International Fluid Power Symposium, Sheffield, England, Paper B2, pp. 21–28.
[128] Zhang, J. H., Chen, Y., Xu, B., Pan, M., and Chao, Q., 2018, "Effects of the splined shaft bending rigidity on the cylinder tilt behaviour for high-speed electro-hydrostatic actuator pumps," Chin. J. Aeronaut., https://doi.org/10.1016/j.cja.2018.03.007.
[129] Kim, J. K., and Jung, J. Y., 2002, "Fluid film measurements on the spherical valve plate in oil hydraulic axial piston pumps," 2nd Asia International Conference on Tribology, Jeju Island, Korea, pp. 381–382.
[130] Kim, J. K., Kim, H. E., Lee, Y. B., Jung, J. Y., Oh, S. H., 2005, "Measurment of fluid film thickness on the valve plate in oil hydraulic axial piston pumps (Part II: Spherical design effects)," J. Mech. Sci. Technol., **19**(2), pp. 655–663.
[131] Kazama, T., 2010, "Thermohydrodynamic lubrication model applicable to a slipper of swashplate type axial piston pumps and motors (Effects of operating conditions)," Tribol. Online, **5**(5), pp. 250–254.
[132] Kazama, T., Suzuki, M., and Suzuki, K., 2015, "Relation between sliding-part temperature and clearance shape of a slipper in swashplate axial piston motors," JFPS Int. J. Fluid Power Syst., **8**(1), pp. 10–17.
[133] Anderson, J. A., 1991, "Variable displacement electro-hydrostatic actuator," IEEE 1991 National Aerospace and Electronics Conference, Dayton, Ohio, USA, pp. 529–534.
[134] Chen, W. Z., Lin, T., Hill, B. P., and Brown, J. R., 1995, "Thermal modeling of a flight-critical electrohydrostatic actuator," SAE Technical Paper No. 951403.
[135] Song, Z. N., Jiao, Z. X., Shang, Y. X., Wu, S., and Hu, W. N., 2015, "Design and analysis of a direct load sensing electro-hydrostatic actuator," 2015 International Conference on Fluid Power and Mechatronics, Harbin, China, pp. 624–627.
[136] Hu, W. N., Zhou, L., Tian, Y. S., Jiao, Z. X., Shang, Y. X., Song, Z. N., and Yan, L., 2015, "Analysis for the power loss of electro hydrostatic actuator and hydraulic actuator," 2015 IEEE International Conference on Advanced Intelligent Mechatronics, Busan, Korea, pp. 613–616.
[137] Shang, L., and Ivantysynova, M., 2015, "Port and case flow temperature prediction for axial piston machines," Int. J. Fluid Power, **16**(1), pp. 35–51.
[138] Halat, J. A., 1985, "Hydraulic pumps for high pressure non-flammable fluids," SAE Technical Paper No. 851911.
[139] Schenk, A., Zecchi, M., and Ivantysynova, M., 2013, "Accurate prediction of axial piston machine's performance through a thermo-elasto-hydrodynamic simulation model," ASME/BATH 2013 Symposium Fluid Power Motion Control, Sarasota, Florida, USA.
[140] Zhang, J. H., Li, Y., Xu, B., Chen, X., and Pan, M., 2018, "Churning losses analysis on the thermal-hydraulic model of a high-speed electro-hydrostatic actuator pump," Int. J. Heat Mass Transf., **127**, pp. 1023–1030.
[141] Olsson, H., 2003, "Power losses in an axial piston pump used in industrial hydrostatic transmissions," 8th Scandinavian International Conference on Fluid Power, Tampere, Finland.
[142] Zhang, J. H., Li, Y., Xu, B., Pan, M., and Lv, F., 2017, "Experimental study on the influence of the rotating cylinder block and pistons on churning losses in axial piston pumps," Energies, **10**(5), p. 662.
[143] Xu, B., Zhang, J. H., Li, Y., and Chao, Q., 2015, "Modeling and analysis of the churning losses characteristics of swash plate axial piston pump," 2015 International Conference on Fluid Power and Mechatronics, Harbin, China, pp. 22–26.
[144] Zecchi, M., Mehdizadeh, A., and Ivantysynova, M., 2013, "A novel approach to predict the steady state temperature in ports and case of swash plate type axial piston machines," 13th Scandinavian International Conference on Fluid Power, Linköping, Sweden, pp. 177–187.
[145] Ivantysyn, R., and Weber, J., 2018, "Investigation of the thermal behaviour in the lubricating gap of an axial piston pump with respect to lifetime," 11th International Fluid Power Conference, Aachen, Germany, Vol. 2, pp. 68–83.
[146] Ma, J. M., Chen, J., Li, J., Li, Q. L., and Ren, C. Y., 2015, "Wear analysis of swash plate/slipper pair of axis piston hydraulic pump," Tribol. Int., **90**, pp. 467–472.
[147] Lamb, W. S., 1987, "Cavitation and aeration in hydraulic systems," BHRA, The Fluid Engineering Center.
[148] Hashemi, S., Kroker, A., Bobach, L., and Bartel, D., 2016, "Multibody dynamics of pivot slipper pad thrust bearing in axial piston machines incorporating thermal elastohydrodynamics and mixed lubrication model," Tribol. Int., **96**, pp. 57–76.
[149] Pelosi, M., and Ivantysynova, M., 2011, "The influence of pressure and thermal deformation on the piston/cylinder interface film thickness," 52nd National Conference on Fluid Power, Las Vegas, Nevada, USA, pp. 227–236.
[150] Pelosi, M., and Ivantysynova, M., 2012, "Heat transfer and thermal elastic deformation analysis on the piston/cylinder interface of axial piston machines," ASME J. Tribol., **134**(4), p. 041101.

[151] Li, Y. H., Ji, Z. L., Yang, L. M., Zhang, P., Xu, B., and Zhang, J. H., 2017, "Thermal-fluid-structure coupling analysis for valve plate friction pair of axial piston pump in electrohydrostatic actuator (EHA) of aircraft," Appl. Math. Model, **47**, pp. 839–858.
[152] Zecchi, M., and Ivantysynova, M., 2012, "Cylinder block/valve plate interface–a novel approach to predict thermal surface loads," 8th International Fluid Power Conference, Dresden, Germany, pp. 285–298.
[153] Ivantysynova, M., and Lasaar, R., 2004, "An investigation into micro- and macrogeometric design of piston/cylinder assembly of swash plate machines," Int. J. Fluid Power, **5**(1), pp. 23–36.
[154] Garrett, R. A., 2009, "Investigation of reducing energy dissipation in axial piston machines of swashplate type using axially waved pistons," M.S. Thesis, Purdue University, USA.
[155] Gels, S., and Murrenhoff, H., 2010, "Simulation of the lubricating film between contoured piston and cylinder," Int. J. Fluid Power, **11**(2), pp. 15–24.
[156] Wondergem, A., 2014, "Piston/cylinder interface of axial piston machines-effect of piston micro-surface shaping," M.S. Thesis, Purdue University, USA.
[157] Wondergem, A., and Ivantysynova, M., 2014, "The impact of the surface shape of the piston on power losses," 8th FPNI Ph.D. Symposium on Fluid Power, Lappeenranta, Finland.
[158] Wondergem, A., and Ivantysynova, M., 2015, "The impact of micro-surface shaping on the piston/cylinder interface of swash plate type machines," ASME/BATH 2015 Symposium Fluid Power Motion Control, Chicago, Illinois, USA.
[159] Wondergem, A., and Ivantysynova, M., 2016, "The impact of micro-surface shaping of the piston on the piston/cylinder interface of an axial piston machine," 10th International Fluid Power Conference, Dresden, Germany, Vol. 2, pp. 289–300.
[160] Ernst, M. H., and Ivantysynova, M., 2017, "Cylinder bore micro-surface shaping for high pressure axial piston machine operation using water as hydraulic fluid," ASME/BATH 2017 Symposium on Fluid Power and Motion Control, Sarasota, Florida, USA.
[161] Ivantysynova, M., and Baker, J., 2009, "Power loss in the lubricating gap between cylinder block and valve plate of swash plate type axial piston machines," Int. J. Fluid Power, **10**(2), pp. 29–43.
[162] Chacon, R., and Ivantysynova, M., 2014, "An investigation of the impact of micro surface on the cylinder block/valve plate interface performance," 8th FPNI Ph.D. Symposium on Fluid Power, Lappeenranta, Finland.
[163] Chacon, R., 2014, "Cylinder block/valve plate interface performance investigation through the introduction of micro-surface shaping," M.S. Thesis, Purdue University, USA.
[164] Leonhard, L., and Murrenhoff, H., 2010, "Deterministic surface texturing for the tribologic contacts in hydrostatic machines," 7th International Fluid Power Conference, Aachen, Germany, pp. 49–59.
[165] Murrenhoff, H., Eneke, C., Gels, S., Heipl, O., Leonhard, L., Schumacher, J., and Wohlers, A., 2010, "Efficiency improvement of fluid power components focusing on tribological systems," 7th International Fluid Power Conference, Aachen, Germany, pp. 215–248.
[166] Wang, Z. Q., Gu, L. Y., and Li, L., 2013, "Experimental studies on the overall efficiency performance of axial piston motor with a laser surface textured valve plate," Proc. Inst. Mech. Eng. Part B: J. Eng. Manuf., **227**(7), pp. 1049–1056.
[167] Chen, Y., Zhang, J. H., Xu, B., Wang, F., and Li, H. Q., 2018, "Investigation of laser surface texturing for integrated PV (pressure×velocity)-value-decreased retainer in an EHA pump," 11th International Fluid Power Conference, Aachen, Germany, Vol. 1, pp. 408–418.
[168] Zhang, J. H., Chen, Y., Xu, B., Chao, Q., Zhu, Y., and Huang, X. C., 2018, "Effect of surface texture on wear reduction of the tilting cylinder and the valve plate for a high-speed electro-hydrostatic actuator pump," Wear, **414**–**415**, pp. 68–78.
[169] van Bebber, D., and Murrenhoff, H., 2002, "Improving the wear resistance of hydraulic machines using PVD-coating technology," O+ P Ölhydraulik und Pneumatik, **46**(11–12), pp. 1–35.
[170] Murrenhoff, H., and Scharf, S., 2006, "Wear and friction of ZRCG-coated pistons of axial piston pumps," Int. J. Fluid Power, **7**(3), pp. 13–20.
[171] Enekes, C., and Murrenhoff, H., 2008, "Efficiency of axial piston pumps with coated tribological systems," International Symposium on Friction, Wear, and Wear Protection, Aachen, Germany, pp. 575–581.
[172] Enekes, C., Murrenhoff, H., Dott, W., and Bressling, J., 2010, "Tribological and ecotoxicological behaviour of a synthetic ester and its effect on friction and wear in axial piston pumps," 7th International Fluid Power Conference, Aachen, Germany.
[173] Enekes, C., and Murrenhoff, H., 2010, "How environmentally friendly tribological systems influence the efficiency of axial piston machines," Tribol. Online, **5**(5), pp. 245–249.
[174] Murrenhoff, H., Enekes, C., Gold, P. W., Jacobs, G., Rombach, V., Plogmann, M., Bobzin, K., Bagcivan, N., Theiß, S., and Goebbels, N., 2010, "Environmentally friendly tribological systems in axial piston machines," 17th International Colloquium Tribology 2010 – Solving Friction and Wear Problems, Ostfildern, Germany, pp. 777–780.
[175] Rahmfeld, R., Marsch, S., Göllner, W., Lang, T., Dopichay, T., and Untch, J., 2012, "Efficiency potential of dry case operation for bent-axis motors," 8th International Fluid Power Conference, Dresden, Germany.
[176] Theissen, H., Gels, S., and Murrenhoff, H., 2013, "Reducing energy losses in hydraulic pumps," 8th International Conference on Fluid Power Transmission and Control, Hangzhou, China, pp. 77–81.
[177] Li, Y., Xu, B., Zhang, J. H., and Chen, X., 2018, "Experimental study on churning losses reduction for axial piston pumps," 11th International Fluid Power Conference, Aachen, Germany, Vol. 1, pp. 272–280.

Figure Caption List

Fig. 1 The axial piston pump used in the EHA system: (a) schematic of an EHA system; (b) schematic of an axial piston pump

Fig. 2 Relationship between a maximum rotational speed and a volumetric displacement for three different aerospace pumps [12]

Fig. 3 Cavitation induced by the jet flow: (a) jet flow formed between the cylinder wall and relief groove of the valve plate; (b) detection of the cavitation [31]

Fig. 4 Centrifugal effect on the cylinder pressure in the radial direction [34]

Fig. 5 Experimental results for the relationship between the delivery flow rate and the rotational speed [34]

Fig. 6 Cavitation damage on the components of an axial piston pump: (a) valve plate [36], (b) cylinder block [41], (c) slipper

Fig. 7 Spherical design for the cylinder block bottom surface to reduce pressure losses: (a) velocity of the hydraulic fluids entering the cylinder chamber; (b) comparison of the circumferential velocity between the spherical and flat designs for the cylinder block bottom surface

Fig. 8 Schematic of the pre-expansion volume (PEV) [56]

Fig. 9 Valve plate with damping hole at the relief groove: (a) effect of the damping hole on the jet flow; (b) photograph of the valve plate with damping hole after a 1000 h endurance test [33]

Fig. 10 Cross angle in an axial piston pump [84]

Fig. 11 Schematic of three types of check valves: (a) simple check valve [59]; (b) highly dynamic control valve [78]; (c) heavily damped check valve (HDCV) [89]

Fig. 12 The in-built pulsation attenuator in an aviation pump [93]

Fig. 13 Comparison between standard and "male" slippers: (a) standard "female" slipper; (b) "male" slipper

Fig. 14 Comparison between positive-force and fixed-clearance retaining mechanisms: (a) positive-force retaining mechanism; (b) fixed-clearance retaining mechanism

Fig. 15 Comparison between three types of pistons [111]: (a) hollow piston; (b) capped piston; (c) filled piston

Fig. 16 Tilting motion of the cylinder block due to the centrifugal effect

Fig. 17 Insert in the pump casing to reduce churning loss [176]: (a) configuration of an insert; (b) effect of the insert on the turbulent flow in a pump casing